Structure-Based Mechanism of O_2 Sensing and Ligand Discrimination by the FixL Heme Domain of *Bradyrhizobium japonicum*[†,‡]

Bing Hao,[§] Clara Isaza,[||] Joseph Arndt,[§] Michael Soltis,[⊥] and Michael K. Chan*[,§]

Departments of Biochemistry and Chemistry, and The Ohio State Biophysics Program, The Ohio State University, 484 West 12th Avenue, Columbus, Ohio 43210, and The Stanford Synchrotron Research Laboratory, SLAC, P.O. Box 4349, Bin 99, Stanford University, Stanford, California 94309

Received February 19, 2002; Revised Manuscript Received August 15, 2002

ABSTRACT: Structures of the *Bradyrhizobium japonicum* FixL heme domain have been determined in the absence and presence of specific ligands to elucidate the detailed features of its O_2 sensing mechanism. The putative roles of spin-state and steric hindrance were evaluated by the structure determination of ferrous CO-bound BjFixLH and correlating its features with other ligand-bound structures. As found for NO-BjFixLH, no protein conformational change was observed in CO-BjFixLH, suggesting a more complicated mechanism than solely spin state or ligand sterics. To evaluate the role of oxidation state, the structure of the ferrous deoxy-BjFixLH was determined. The structure of deoxy-BjFixLH was found to be virtually identical to the structure of the ferric met-BjFixLH. The role of hydrogen bonding of substrates to a heme-pocket water was evaluated by determining the structure of BjFixLH bound to 1-methyl-imidazole that cannot form a hydrogen bond with this water. In this case, the heme-mediated conformational change was observed, limiting the potential importance of this interaction. Finally, the structure of cyanomet-BjFixLH was revisited to rule out concerns regarding the partial occupancy of the cyanide ligand in a previous structure. In the revised structure, Arg 220 was found to move into the heme pocket to form a hydrogen bond to the bound cyanide ligand. The implications of these results on FixL's sensing mechanism are discussed.

Heme protein sensors are a class of enzymes that regulate DNA binding and enzymatic activities in response to the presence of gaseous diatomics—CO, NO, and O_2 (*1*−*3*). As sensors, these heme proteins must be able to discriminate their target ligands from those of similar size and shape to induce their ligand specific functional activities. Hence, critical issues in the study of heme protein sensors are the details for how each of the key features of sensing (recognition, discrimination, and allostery) is achieved.

One class of heme proteins where these issues are important is the FixL proteins of *Rhizobia.* Each FixL serves as an O_2 sensor that, together with an associated two-component response regulator, FixJ, controls the transcription of nitrogen fixation genes (*4*−*7*). FixL proteins are comprised of two domains, an N-terminal heme-containing PAS domain that serves as the oxygen-sensing element and a C-terminal histidine kinase domain whose activity is regulated by the heme domain (*8*). In the absence of dioxygen, the histidine kinase is active ("on") and transfers the phosphoryl group to FixJ that initiates the nitrogen fixation gene expression. In the presence of dioxygen, the histidine kinase activity is turned "off". How dioxygen binding regulates the allostery both within the heme domain and between the heme domain and its associated histidine kinase are two of the fundamental questions related to this protein.

Some of these issues have been addressed by structural studies of the *Bradyrhizobium japonicum* FixL heme domain (BjFixLH)[1] (*9*, *10*). These studies reveal a mechanism of a heme-driven conformational change that is distinct from classical globins. Unlike hemoglobin, the movement of the proximal histidine and its associated α-helix does not play a major role in FixL's allosteric mechanism. Instead, binding of dioxygen to the FixL heme results in the flattening of the heme porphyrin and the shift of a critical loop, the FG loop (residues Thr 209 to Arg 220), away from the heme pocket (*9*, *10*). This FG loop shift presumably induces a global conformational change in the full-length protein that in turn inhibits the kinase activity. While cyanide and imidazole

[†] This work was supported by funds from the American Heart Association, Ohio Division (9960377V), and from a fellowship from the Alfred P. Sloan Foundation.

[‡] The coordinates have been deposited in the Protein Data Bank. PDB filenames: 1LSV (CO-BjFixLH), 1LSW (deoxy-BjFixLH), 1LSX (MeIm-BjFixLH), and 1LT0 (cyanomet-BjFixLH).

* To whom correspondence should be addressed. Phone: (614) 292-8375. FAX: (614) 292-6773. E-mail: chan@chemistry.ohio-state.edu.

[§] Departments of Biochemistry and Chemistry, The Ohio State University.

[||] The Ohio State Biophysics Program, The Ohio State University.

[⊥] The Stanford Synchrotron Research Laboratory, Stanford University.

[1] Abbreviations: BjFixL, *Bradyrhizobium japonicum* FixL; BjFixLH, BjFixL heme domain; RmFixL, *Rhizobium meliloti* FixL; RmFixLT, soluble truncated form of RmFixL containing both heme and kinase domains; RmFixLH, RmFixL heme domain; met-RmFixLH, unliganded ferric RmFixLH; oxy-RmFixLH, RmFixLH bound to dioxygen; deoxy-BjFixLH, unliganded ferrous BjFixLH; met-BjFixLH, unliganded ferric BjFixLH; oxy-BjFixLH, ferrous BjFixLH bound to dioxygen; cyanomet-BjFixLH, ferric BjFixLH bound to cyanide; CO-BjFixLH, ferrous BjFixLH bound to carbon monoxide; NO-BjFixLH, ferrous BjFixLH bound to nitric oxide; imidazole-BjFixLH, ferric BjFixLH bound to imidazole; MeIm-BjFixLH, ferric BjFixLH bound to 1-methyl-imidazole.

10.1021/bi020144l CCC: $22.00
Published on Web 10/04/2002

were found to also induce this conformational change, nitric oxide did not (*9*, *10*).

Despite the structure determination of the heme domains of both BjFixLH and the *Rhizobium meliloti* FixL heme domain (RmFixLH), there still remains controversy regarding the mechanism of the heme-driven conformational change. In hemoglobins, the change of the heme iron from high spin to low spin upon dioxygen binding plays an important role in the allosteric mechanism (*11*, *12*). Due to its smaller size, the low-spin iron can move into the plane of the porphyrin ring, thus causing a shift of its attached proximal histidine and its associated F-helix. On the basis of the observation that the inhibition of FixL's kinase activity is linked to the binding of the strong-field ligands for both ferric and ferrous oxidation states, a spin-state model was suggested. Here, the change in the spin-state of the heme iron is proposed to be the driving force for the conformational change (*13*).

Others have argued that the sterics of the ligand is the driving force for the conformational change based on data suggesting a tight heme distal pocket and FixL's fast on-rates for imidazole binding (*14*). This model has also been supported by mutagenesis experiments, but these data appear inconclusive. Mutation of the distal residues Ile 209 and Ile 210 in the FG loop (corresponding to Ile 215 and Ile 216 in BjFixL) to Ala, His, and Trp have been shown to lead to an increase in the kinase autophosphorylation activity for both deoxy− and oxy-RmFixLT (*15*). This result has been used to suggest that these residues play an important role in FixL's O_2-sensing mechanism. The steric interaction between these residues and the bound dioxygen ligand is proposed to be the driving force of the conformational change. While this argument makes sense for the Ala mutations, the data appear inconsistent for the His and Trp mutants. Both His and Trp are larger than Ile and thus should lead to down regulation if the steric hindrance model is correct.

EXAFS studies have been used to suggest the involvement of the proximal side of the heme (*16*). The distance between the heme plane (Ct) and the nitrogen atom of the proximal histidine (Nim) was found to correlate with the kinase activity. Oxy- and cyanomet-RmFixLT exhibited short Ct−Nim distances and no kinase activity, while the met-, ferric fluoride, and deoxy- forms were found to have longer distances and reasonable kinase activity. This was used to suggest that the movement of the proximal histidine plays a role in the signal transduction between the heme and kinase domains. It should be noted, however, that no movement of the proximal histidine has been observed in any of our ligand-bound structures. Instead, while closer Ct−Nim distances are observed for oxy-BjFixLH and other on-state structures, these result from the flattening of the heme ligand.

In an attempt to resolve how these and other features are used by FixL to recognize and discriminate O_2 from other ligands, the structures of met-BjFixLH, as well as a series of ligand-bound BjFixLH complexes, have been determined (*9*, *10*). As part of this continuing analysis, we report here the first structures of the unliganded ferrous BjFixLH (deoxy-BjFixLH), BjFixLH bound to carbon monoxide (CO-BjFixLH), and 1-methyl-imidazole (MeIm-BjFixLH) and revisit the structure of BjFixLH bound to cyanide (cyanomet-BjFixLH). These structures and our previously determined met−, oxy−, NO−, and imidazole-BjFixLH structures have been used to develop a mechanism of ligand discrimination and allostery within the heme domain.

MATERIALS AND METHODS

Crystallization and Data Collection. Met-BjFixLH crystals were prepared as reported previously (*9*). CO-BjFixLH crystals were generated by using a MRC Cryo-Xe−Siter at the beamline 9−2 at Stanford Synchrotron Radiation Laboratory (SSRL). The met-BjFixLH crystals were transferred stepwise to anaerobic synthetic mother liquor containing increasing concentrations of glycerol (up to 30% (vol/vol)) and then soaked in a solution containing saturated sodium dithionite for several minutes. The reduced crystals were then mounted on a cryo-loop and pressurized in the Cryo-Xe-Siter under a CO pressure of 300 psi for 70 min. The CO-BjFixLH crystals were flash-cooled under pressure in liquid carbon tetrafluoride. Deoxy-BjFixLH crystals were obtained by soaking crystals with degassed synthetic mother liquor containing saturated sodium dithionite. Upon treatment, the color of the reduced crystals changed from orange-red to cherry-red within several minutes. They were then flash-cooled in liquid nitrogen for data collection. MeIm-BjFixLH crystals were prepared by soaking met-BjFixLH crystals in synthetic mother liquor containing 200 mM 1-methyl-imidazole for 90 min. The cyanomet-BjFixLH crystals were obtained either directly by growing the crystal with 10mM potassium cyanide or by treating met-BjFixLH crystals with 100 mM potassium cyanide for 30 min. Both ligand-bound forms were transferred gradually to synthetic mother liquor solutions containing ligand (1-methyl-imidazole or cyanide) and increasing concentrations of glycerol up to 30% prior to being flash-cooled in liquid nitrogen. The diffraction data were collected at 100 K with the ADSC-Q4 CCD detector (Table 1). Data processing and reduction were performed using DENZO and SCALEPACK (*17*).

Structure Determination and Refinement. The structures of deoxy-BjFixLH and each of the ligand-bound complexes were determined using the met-BjFixLH structure (PDB entry: 1DRM) as the starting model. Model building and refinement were performed using the programs O (*18*) and X-PLOR 3.851 (*19*), respectively. A flat bulk solvent correction and an overall anisotropic *B*-factor scaling were applied to the diffraction data. The ligands, solvent molecules, and the residues forming the FG loop were modeled based on the resulting $2F_O-F_C$ and F_O-F_C electron density maps. The quality of the model for each structure was evaluated using PROCHECK (*20*). All stereochemical parameters for each structure were within acceptable ranges with majority being better than acceptable. Figures were prepared using the programs Molscript (*21*), Raster3D (*22*), and XtalView (*23*). The root-mean-square deviations (RMSD) after least-squares fitting of the overall, main-chain, and heme atoms of deoxy- and each of the six ligand-bound structures (CO-, NO-, cyanomet-, imidazole-, MeIm-, and oxy-BjFixLH) to met-BjFixLH were determined using the program CNS (*24*).

RESULTS AND DISCUSSION

Previous studies demonstrated that the FixL heme domain belongs to the PAS superfamily, a family of proteins that adopts a glove-like fold consisting of a central β-sheet with

Table 1: Data Processing and Refinement Statistics[a]

crystals	CO	cyanomet[b]	cyanomet[c]	MeIm	deoxy
space group	*R*32	*R*32	*R*32	*R*32	*R*32
wavelengths (Å)	0.9790	1.4009	1.0000	0.9184	0.9920
cell parameters (Å)	$a = 127.01$	$a = 127.66$	$a = 127.77$	$a = 127.04$	$a = 127.57$
	$c = 58.14$	$c = 58.43$	$c = 58.30$	$c = 58.61$	$c = 58.42$
resolution range (Å)	20.0−2.4	20.0−2.7	20.0−2.4	20.0−2.7	20.0−2.2
no. of reflections	45212	31639	26220	25018	49059
no. of unique reflections	7132	5150	7182	5000	9312
no. of protein (ligand) atoms	966 (2)	973 (2)	964 (2)	957 (6)	966
no. of solvent molecules	38	36	36	50	45
B-factor of protein (Å^2)	20.6	28.7	18.8	26.2	21.6
B-factor of ligand (Å^2)	12.4	22.8	15.1	17.6	−
completeness (%)[d]	99.8 (96.6)	97.9 (95.3)	96.9 (100.0)	98.7 (90.7)	99.6 (100.0)
I/σ	14.4 (6.8)	16.6 (7.9)	24.3 (7.0)	17.0 (6.5)	15.5 (7.6)
R_{merge} (%)[e]	4.4 (31.5)	4.7 (25.8)	3.2 (22.1)	4.7 (21.7)	4.4 (29.1)
R factor (%)[f]	21.5	21.0	22.6	20.1	22.1
R_{free} (%)[g]	25.1	24.7	26.8	22.9	26.5
RMSD of bond distance (Å)	0.014	0.013	0.016	0.013	0.014
RMSD of bond angles (deg)	1.68	1.62	1.73	1.55	1.57

[a] The CO-BjFixLH data were collected on beamline 9-2 at SSRL. The cyanomet-BjFixLH data were collected on X4A at the National Synchrotron Light Source in Brookhaven National Laboratory. The MeIm-BjFixLH data were collected on BIOCARS 14D at the Advance Photon Source at Argonne National Laboratory. The deoxy-BjFixLH data were collected on beamline 9-1 at SSRL. [b] The crystal was prepared by soaking the met-BjFixLH crystal with 100 mM potassium cyanide. [c] The crystal was grown in synthetic mother liquor containing 10 mM potassium cyanide. [d] The numbers in parentheses are for the highest resolution shell. [e] $R_{merge}(I) = \sum_h \sum_i |I_i - I| / \sum_h \sum_i I$, where I is the mean intensity of the i observations of reflection h. [f] R factor $= 100 \times \sum |F_{obs} - F_{calc}| / \sum |F_{obs}|$, where F_{obs} and F_{calc} are the observed and calculated structure factors, respectively. [g] R_{free} was calculated using 8% of reflections.

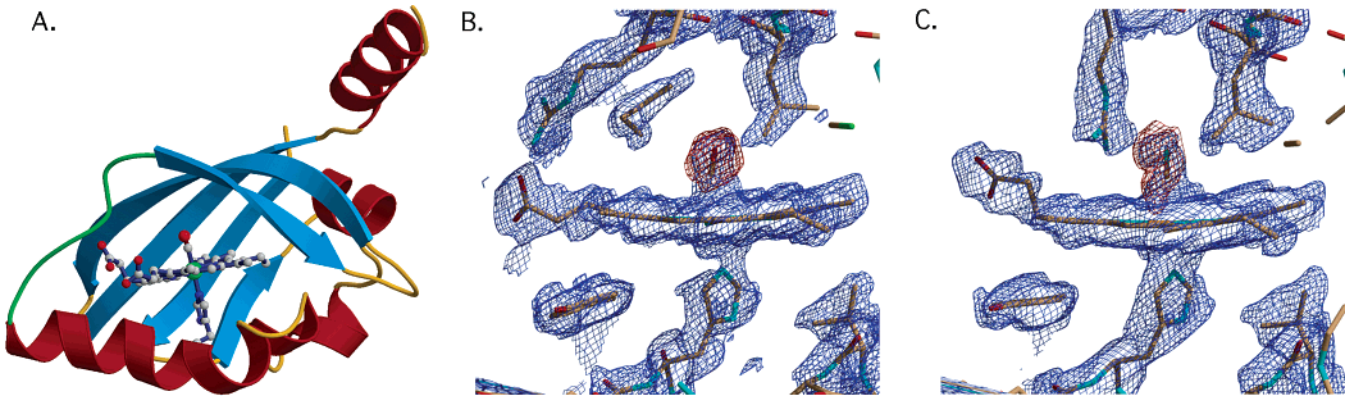

FIGURE 1: (A) Ribbons diagram of CO-BjFixLH colored by secondary structure (α-helix, red; β-strand, blue; random coil, tan; the FG loop, green). The atoms of the heme, dioxygen ligand, and proximal histidine are depicted as ball-and-stick models and are colored by element (carbon, gray; oxygen, red; nitrogen, blue; and iron, green). Ball-and-stick models with electron density for the BjFixLH heme-binding pocket of (B) CO-BjFixLH and (C) the revised cocrystallized cyanomet-BjFixLH ($2F_O - F_C$ density (blue, 1.0 σ) and $F_O - F_C$ omit density (red, 3.0 σ)).

flanking α-helices (Figure 1A) (*8*, *25*). The heme cofactor sits in the palm of the glove. All of the BjFixLH structures, including those determined in this study (deoxy-, CO-, MeIm-, and cyanomet-BjFixLH), adopt the same overall fold (*9*, *10*). The major difference between the unbound and certain ligand-bound forms is the position of the FG loop (residues Thr 209 to Arg 220 in BjFixL) (Figures 1−3). In the unliganded met-BjFixLH (on state), the FG loop lies close to the heme pocket (closed conformation) (Figure 2A). In oxy-BjFixLH (off state), the FG loop is shifted away from the heme pocket (open conformation) (Figure 2E).

Structure of CO-BjFixLH: Investigating the Role of Spin-State and Sterics on the Conformational Change. The feature that drives the heme-mediated conformational change in FixL proteins has been an area of great speculation. A spin-state mechanism has been proposed in which the change in the spin state from high spin in the unliganded form to low spin upon binding of dioxygen and other strong-field ligands induces the conformational change (*13*). Consistent with this hypothesis, structures of oxy-BjFixLH and imidazole-BjFixLH exhibit the conformational change (*10*). Alternatively, more recent proposals have suggested a mechanism where the steric hindrance of the bound ligand induces the conformational change (*14*, *26*). This hypothesis is supported by the fast on-rates for imidazole binding.

Strangely, however, neither of these two models is in agreement with the NO-BjFixLH structure (*10*). While NO-BjFixLH would be expected to be low spin, no major conformational change is observed (Figures 2D and 3A,B). Similarly, the NO-BjFixLH structure argues against ligand sterics as the side chain of Ile 238 within the heme pocket simply adjusts to accommodate the bound NO ligand. NO-bound hemes can be unusual, however, since they tend to be distorted. Thus, it could be argued that the features observed in the NO-bound structure could be a consequence of some unusual property of the NO-bound heme (*27*, *28*). Hemes bound to CO, however, should be low spin and yet adopt more typical geometries based on previously deter-

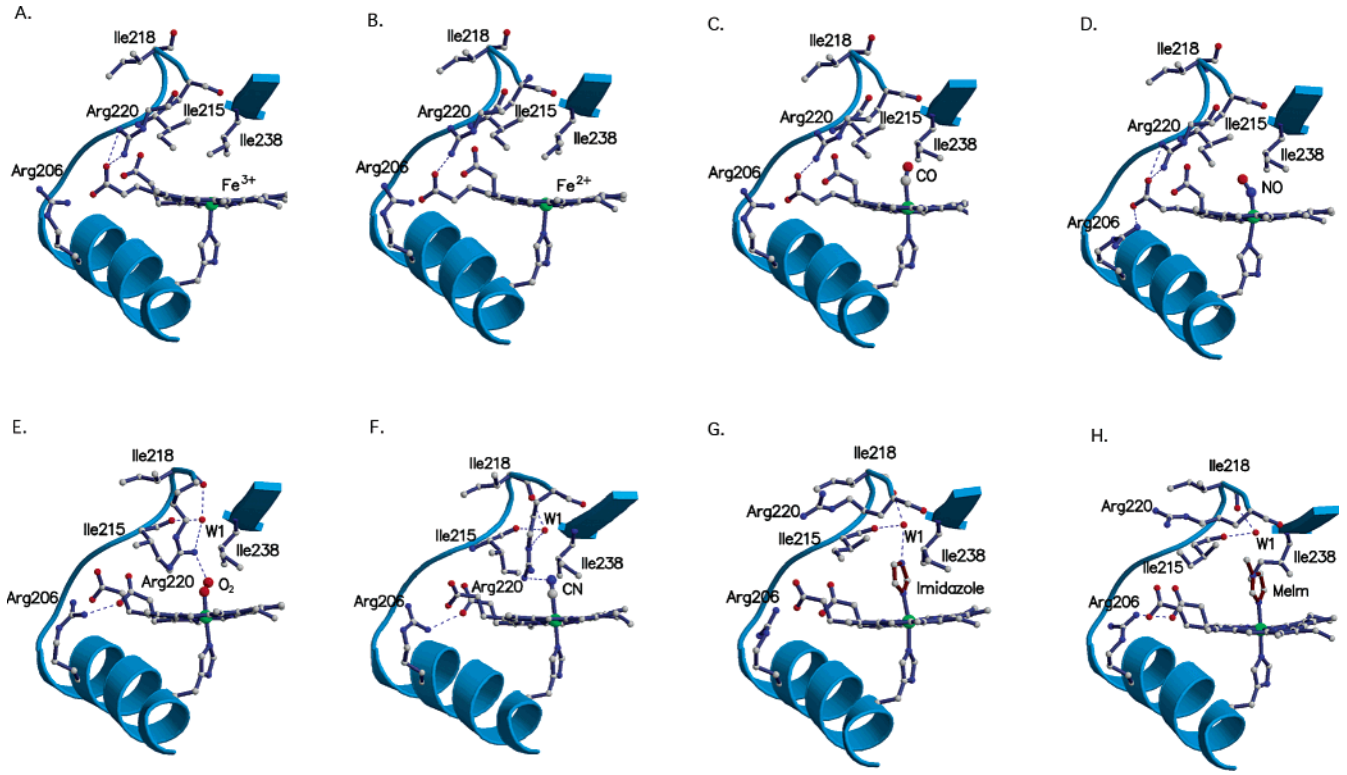

FIGURE 2: Ribbons and ball-and-stick model diagrams of the BjFixLH heme-binding pocket for (A) met-BjFixLH, (B) deoxy-BjFixLH, (C) CO-BjFixLH, (D) NO-BjFixLH, (E) oxy-BjFixLH, (F) the revised cocrystallized cyanomet-BjFixLH, (G) imidazole-BjFixLH, and (H) MeIm-BjFixLH. W1 represents water. The dash lines show the hydrogen bonding or the salt-bridge interactions.

mined structures of globins and porphyrin model compounds (*29*, *30*). Hence, to evaluate the roles of spin state and sterics in the mechanism of FixL's conformational change, the structure of ferrous CO-BjFixLH was determined.

It was surprisingly difficult to obtain suitable crystals of CO-BjFixLH in light of the ease of preparing crystals of oxy-BjFixLH. After numerous trials, suitable crystals were obtained via the anaerobic reduction of met-BjFixLH crystals with dithionite followed by a long-term incubation under a high-pressure CO atmosphere. The structures of the overall protein and the heme-binding pocket for CO-BjFixLH are shown in panels A and B, respectively, of Figure 1. Importantly, F_O-F_C and $2F_O-F_C$ electron density maps clearly show the presence of the CO molecule (Figure 1B), but no shift of the FG loop is observed. The overall RMSD of the main-chain atoms between CO-BjFixLH and met-BjFixLH is only 0.27 Å, which is the smallest deviation observed for all the ligand-bound forms that have been determined (Figure 3B). Analysis of the side chains reveals only subtle differences in the positions of Asp 212 and Ile 238. The side chain of Asp 212 is shifted away from its salt-bridge with Arg 206 (Figure 2A and 2C), while Ile 238 is in the same position as that found in oxy-, NO-, and imidazole-BjFixLH. The shift of Ile 238 likely results from the steric interaction required to accommodate the CO ligand. Because CO is a strong-field ligand and its binding does not induce the conformational change, these data suggest that neither sterics of the ligand itself nor the change of the spin state of the heme iron is sufficient to drive the conformational change.

Role of Arg 220 as a Steric Barrier: Revisiting the Structure of Cyanomet-BjFixLH. As the CO-BjFixLH and NO-BjFixLH data suggested that the mechanism for the heme-driven conformational change could be more complex than a simple spin-state or ligand sterics, the previously determined oxy-BjFixLH structure was examined to look for other feature that could be important for inducing the conformational change. One feature of the oxy-BjFixLH structure that stood out was the rotation of Arg 220 into the heme pocket (Figure 2E). The mutagenesis studies by Mukai et. al. suggested that the steric effects of Ile 209 and Ile 210 of RmFixL (corresponding to Ile 215 and Ile 216 in BjFixL) are important for inducing the heme conformational change (*15*). While the CO-BjFixLH structure suggested that sterics of the ligand could not be the factor driving the conformational change, we noted that the movement of Arg 220 into the heme pocket could also provide an alternative steric barrier that could stabilize the off state of the enzyme. One initial concern with this hypothesis was that imidazole-BjFixLH reveals a conformational change, but here Arg 220 did not move into the heme pocket. Comparison of imidazole-BjFixLH and oxy-BjFixLH structures, however, revealed that the imidazole ligand was positioned in the similar orientation as the arginine guanidinium and thus could serve as its own steric barrier (Figure 2E,G).

Another concern with the proposed role of Arg 220 as a steric barrier was the fact that our previous structure of cyanomet-BjFixLH revealed a ligand-induced conformational change of the FG loop, but no movement of Arg 220 into the heme pocket (*9*). We noted recently that the shift of the FG loop in cyanomet-BjFixLH structure was noticeably less than that in oxy- and imidazole-BjFixLH. Thus, we became concerned that the previous cyanomet-BjFixLH structure was based on an average of the on and off states (*10*). To alleviate these concerns, the cyanomet-BjFixLH structure was re-evaluated using crystals that were either soaked at 10-times

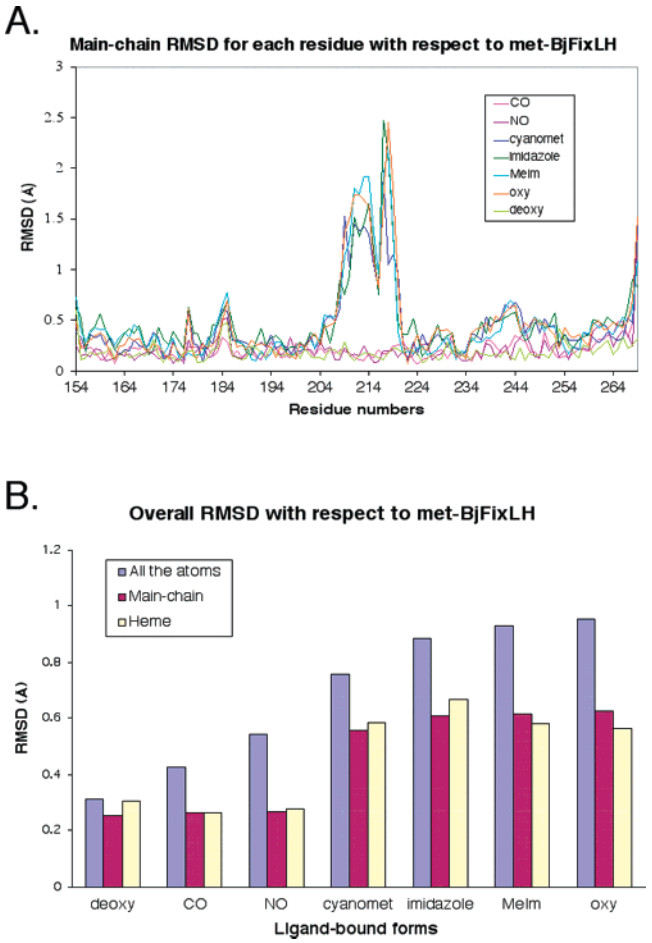

FIGURE 3: Plots of RMSD following least-squares fitting of deoxy- and each of the six ligand-bound structures (CO-, NO-, cyanomet-, imidazole-, MeIm-, and oxy-BjFixLH) to met-BjFixLH: (A) The RMSD for each residue based on its main-chain atoms and (B) the overall RMSD for each structure based on all the atoms, the main-chain atoms, and the heme.

higher cyanide concentrations or crystallized in the presence of cyanide to ensure complete binding.

The two new cyanomet-BjFixLH structures are virtually identical. Both reveal that Arg 220 does move into the heme pocket to form an electrostatic interaction with the bound cyanide and exhibit FG loop shifts that are comparable to oxy-BjFixLH (Figures 1C, 2F, and 3). This observation is significant since it provides support for the correlation of the shift of the FG loop and the rotation of Arg 220 into the heme pocket to presumably serve as a steric barrier for the conformational change. The only exception is imidazole-BjFixLH, but here, the bound imidazole can serve as the steric barrier. To accommodate either Arg 220 or imidazole in the heme pocket, Ile 215 must move away from the heme in a manner that is consistent with the FG loop shift (Figure 2). In the CO- and NO-BjFixLH structures, no conformational change is observed, and Arg 220 remains the same position as that in met-BjFixLH, presumably because the electrostatic interactions between Arg 220 and these ligands are weaker. This would be consistent with the relative electrostatic stabilizations provided by the distal histidine in myoglobins (*31*).

These data suggest the possibility that hydrogen bonding is used by FixL to discriminate O_2 from similarly sized heme ligands such as CO and NO. Hydrogen bonding to a bound dioxygen ligand by either a distal histidine, arginine, or glutamine is also a conserved feature of globins (*11*, *12*, *32*, *33*). This suggests that hydrogen bonding is a common feature utilized by all O_2-binding heme proteins to discriminate O_2 from other ligands (*34*). It should be noted that Arg 220 must be released from its salt bridge with heme proprionate 7 before it can rotate into the heme pocket. This feature is presumably facilitated by a flattening of the heme induced by the binding of strong-field ligands (Figure 3B). Thus, FixL may also discriminate dioxygen from other ligands by its ligand-field strength.

Evaluating the Importance of a Hydrogen Bond in the Heme Distal Pocket: The Structure of MeIm-BjFixLH. While examining the possible role of Arg 220 and exogenous imidazole in driving the observed conformational change, we noted another factor that could induce the conformational change. In each of the off-state structures that we have determined, Arg 220 or imidazole was found to form a hydrogen bond to a tightly bound heme-pocket water (W1 in Figure 2). This hydrogen bond completes a network interaction potentially linking the heme iron and the FG loop, and importantly, is not present in any on-state structures. To explore the significance of this hydrogen bond to the conformational change, the structure of BjFixLH bound to 1-methyl-imidazole was determined. 1-Methyl-imidazole is analogous to imidazole, except that the NH hydrogen is replaced by a methyl group and thus is incapable of hydrogen-bonding the heme-pocket water.

The structure of MeIm-BjFixLH was determined to 2.7 Å resolution. The ligand binds in a fashion similar to imidazole, except that the orientation of the imidazole is rotated by 180° around Fe−N bond. This directs the methylated nitrogen away from the heme pocket and places the C5 carbon in the position where hydrogen bonding usually occurs (Figure 2H). This ring carbon cannot form a hydrogen bond with the conserved water in the heme pocket. The structure reveals that despite the loss of the hydrogen bond to the water, the conformational change still takes place. These data rule out the direct significance of this hydrogen bond in the conformational change.

Structure of Deoxy-BjFixLH: Probing the Role of the Oxidation State of the Heme Iron on the Protein Conformation. Historically, the oxidation state of the heme iron in FixL has been thought not to influence on the structure of the heme domain as the autophosphorylation activities of both ferric and ferrous forms of FixL were found to be the same (*13*). Recently, however, the turnover of RmFixJ to phospho-RmFixJ by RmFixL was found to depend on the oxidation state of the RmFixL heme, with the ferrous form being 100 times more active (*35*). While this suggests the possibility of redox-dependent differences in the structure of RmFixL, structures of ferrous deoxy-RmFixLH and ferric met-RmFixLH exhibit only minor differences. One possibility, however, is that since no ligand-bound forms of RmFixLH could be prepared, crystal packing forces could be stabilizing the conformation observed in both oxidation states. As conformational changes had been observed in our BjFixLH structures, the structure of deoxy-BjFixLH was determined to examine this issue.

Deoxy-BjFixLH crystals were prepared by soaking met-BjFixLH crystals with sodium dithionite. A rapid color

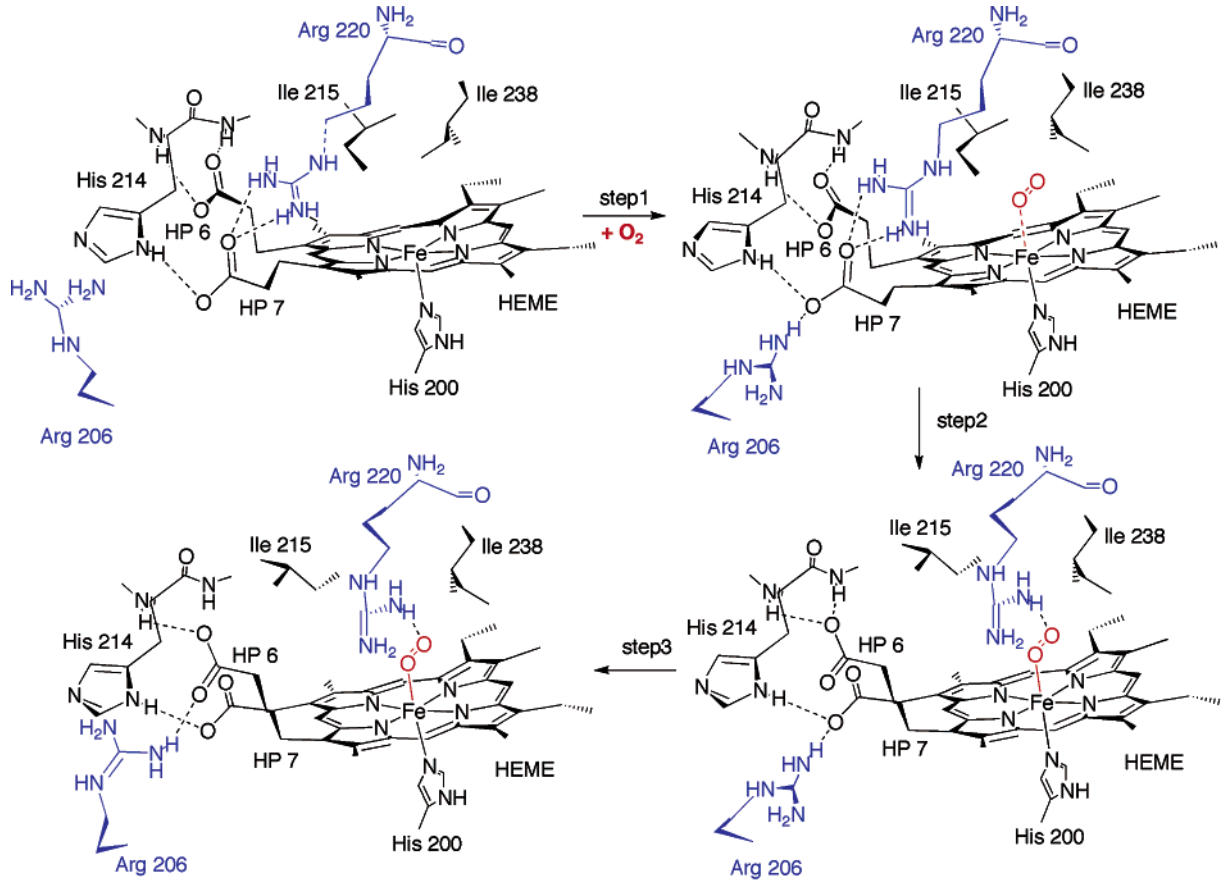

FIGURE 4: Proposed mechanism for the heme-driven conformational change of BjFixLH. The heme-propionates 6 and 7 are labeled HP6 and HP7, respectively. Arg 220 and Arg 206 are colored in blue and dioxygen in red.

change was observed. The overall structure of deoxy-BjFixLH is virtually identical to met-BjFixLH (Figure 3B). On the basis of main-chain atoms, deoxy-BjFixLH has the smallest RMSD to met-BjFixLH of all of the BjFixLH structures we have determined. The heme-binding pocket for deoxy-BjFixLH, shown in Figure 2B, overlaps with that of the met-BjFixLH. The only subtle difference around the heme pocket lies in the interaction between the heme-propionate 6 and Arg 206. In met-BjFixLH, the heme-propionate 6 and Arg 206 are hydrogen-bonded via a water molecule. In deoxy-BjFixLH, this water molecule is missing, and this long-range interaction is lost. The similarity of these structures suggests that if there are oxidation state dependent conformations of the heme domain, either the kinase domain and/or complexation with FixJ is required to induce these differences.

While our structures reveal no differences in the ferric and ferrous states of the heme domain, one observation that may be consistent with the presence of certain subtle differences in their properties has been the apparent difficulty in preparing ligand-bound forms of ferrous BjFixLH. This contrasts the relative ease of preparing ligand bound forms of ferric BjFixLH. While the origin of these differences is unclear, we note that this could partially stem from the fact that ferric iron is smaller than ferrous iron and thus would lead to flattening of the heme and, as a result, would facilitate the binding of ligands to the open axial site. We note that if such an oxidation state dependence existed, it would promote the binding of O_2, which can partially oxidize the heme iron, relative to ligands, such as CO and NO, that do not. Clearly other data will be required to clarify whether oxidation state is indeed a factor in facilitating ligand discrimination of O_2.

A Proposed Mechanism for Ligand Discrimination by BjFixL. On the basis of these structures, we suggest a mechanism for ligand discrimination and allostery for BjFixL (Figure 4). In this model, binding of strong-field ligands to the heme initiates the conformational change by inducing a flattening of the heme plane. This helps to reduce the strength of the salt-bridge between the critical arginine (Arg 220) and heme-propionate 7 (Figure 4, step 1) and provides a mechanism for discriminating the binding of strong-field ligands, such as dioxygen, from the binding of weak-field ligands. Consistent with the importance of this salt-bridge, a second arginine, Arg 206 in BjFixL, is conserved as a positively charged residue in all PAS heme sensors. When the heme flattens, this arginine can form a salt bridge with the same heme-propionate 7 that interacts with Arg 220. This feature has been observed in the NO-BjFixLH structure, a possible model for the intermediate between the on and off states.

The weakening of the Arg 220/heme-propionate 7 salt bridge has two possible outcomes. If Arg 220 cannot hydrogen bond the bound ligand within the heme pocket, as for CO and NO, or the ligand itself cannot provide its own steric barrier (i.e., imidazole), then no FG loop shift is observed. If, however, Arg 220 can form a hydrogen bond to the bound ligand (O_2, CN^-), then Arg 220 will rotate into the heme pocket where it can serve as a steric hindrance against Ile 215. This stabilizes the off state of the enzyme (Figure 4, step 2). As the final step in this mechanism, Arg

206 shifts to form a salt-bridge to heme-propionate 6 (Figure 4, step 3).

CONCLUSIONS

The deoxy-BjFixLH structure and three ligand-bound structures of BjFixLH described in this paper, together with previously determined ligand-bound structures, suggest a mechanism for a heme-driven conformational change that is distinct from hemoglobin. Despite these differences, the elements involved in driving the allostery and ligand discrimination appear to be the same: spin state, electrostatics, and sterics. On the basis of our current model, the ligand-field strength of dioxygen is used to alter the spin-state of the heme iron that in turn initiates a series of events that results in the release of Arg 220 from its salt-bridge to heme-propionate 7. This arginine can then be used to discriminate O_2 from CO and NO by differentiating the ability of these ligands to hydrogen-bond to the arginine side chain. Sterics become important because movement of this arginine into the heme pocket to form a hydrogen bond with the bound dioxygen ligand puts it in a position to serve as a steric hindrance that stabilizes the off state of the enzyme. It should be emphasized, however, that this is only one possible model. Further study will be required to elucidate the intricacies of the sensing mechanism of these FixL proteins.

ACKNOWLEDGMENT

We thank Drs. Marie A. Gilles-Gonzalez and Vondolee Delgado-Nixon for providing us with purified BjFixLH protein. Portions of this research were carried out at the Stanford Synchrotron Radiation Laboratory, a national user facility operated by Stanford University on behalf of the U.S. Department of Energy, Office of Basic Energy Sciences. The SSRL Structural Molecular Biology Program is supported by the Department of Energy, Office of Biological and Environmental Research, and by the National Institutes of Health, National Center for Research Resources, Biomedical Technology Program, and the National Institute of General Medical Sciences. The use of the Advanced Photon Source is supported by the U.S. Department of Energy, Basic Energy Sciences, Office of Science, under Contract No. W-31-109-Eng-38. Use of the BioCARS Sector 14 is supported by the National Institutes of Health, National Center for Research Resources, under Grant Number RR07707. The X4A beamline at the National Synchrotron Light Source, a Department of Energy facility, is supported by the Howard Hughes Medical Institute.

REFERENCES

1. Rodgers, K. R., Lukat-Rodgers, G. S., and Tang, L. (1999) *J. Am. Chem. Soc. 121*, 11241−11242.
2. Chan, M. K. (2000) *J. Porphyrins Phthalocyanines 4*, 358−361.
3. Chan, M. K. (2001) *Curr. Opin. Chem. Biol. 5*, 216−222.
4. Gilles-Gonzalez, M. A., Ditta, G., and Helinski, D. R. (1991) *Nature 350*, 170−172.
5. Gilles-Gonzalez, M. A., and Gonzalez, G. (1993) *J. Biol. Chem. 268*, 16293−7.
6. Agron, P. G., Ditta, G. S., and Helinski, D. R. (1993) *Proc. Natl. Acad. Sci. U.S.A. 90*, 3506−3510.
7. Gilles-Gonzalez, M. A., Gonzalez, G., Perutz, M. F., Kiger, L., Marden, M. C., and Poyart, C. (1994) *Biochemistry 33*, 8067−73.
8. Taylor, B. L., and Zhulin, I. B. (1999) *Microbiol. Mol. Biol. Rev. 63*, 479−506.
9. Gong, W., Hao, B., Mansy, S. S., Gonzalez, G., Gilles-Gonzalez, M. A., and Chan, M. K. (1998) *Proc. Natl. Acad. Sci. U.S.A. 95*, 15177−15182.
10. Gong, W., Hao, B., and Chan, M. K. (2000) *Biochemistry 39*, 3955−3962.
11. Perutz, M. F. (1979) *Annu. Rev. Biochem. 48*, 327−386.
12. Perutz, M. F. (1989) *Mechanisms of Cooperativity and Allosteric Regulation in Proteins*, Cambridge University Press, Cambridge, U.K.
13. Gilles-Gonzalez, M. A., Gonzalez, G., and Perutz, M. F. (1995) *Biochemistry 34*, 232−236.
14. Perutz, M. F., Paoli, M., and Lesk, A. M. (1999) *Chem. Biol. 6*, R291−R297.
15. Mukai, M., Nakamura, K., Nakamura, H., Iizuka, T., and Shiro, Y. (2000) *Biochemistry 39*, 13810−13816.
16. Miyatake, H., Mukai, M., Adachi, S.-I., Nakamura, H., Tamura, K., Iizuka, T., Shiro, Y., Strange, R. W., and Hasnain, S. S. (1999) *J. Biol. Chem. 274*, 23176−23184.
17. Otwinowski, Z., and Minor, W. (1997) *Methods Enzymol. 276*, 307−326.
18. Jones, T. A., Zou, J. Y., Cowan, S. W., and Kjeldgaard, M. (1991) *Acta Crystallogr. A47*, 110−119.
19. Brünger, A. T. (1993) *Acta Crystallogr. D49*, 24−26.
20. Laskowski, R. A., MacArthur, M. W., Moss, D. S., and Thornton, J. M. (1993) *J. Appl. Crystallogr. 26*, 283−291.
21. Kraulis, P. (1991) *J. Appl. Crystallogr. 24*, 946−950.
22. Merritt, E., and Murphy, M. (1994) *Acta Crystallogr. D50*, 869−873.
23. McRee, D. E. (1993) *Practical Protein Crystallography*, Academic Press, Inc., San Diego.
24. Brünger, A. T., and Warren, G. T. (1998) *Acta Crystallogr. D54*, 905−921.
25. Zhulin, I. B., Taylor, B. L., and Dixon, R. (1997) *Trends Biochem. Sci. 22*, 331−333.
26. Miyatake, H., Mukai, M., Park, S.-Y., Adachi, S.-I., Tamura, K., Nakamura, H., Nakamura, K., Tsuchiya, T., Iizuka, T., and Shiro, Y. (2000) *J. Mol. Biol. 301*, 415−431.
27. Ellison, M. K., and Scheidt, W. R. (1997) *J. Am. Chem. Soc. 119*, 7404−7405.
28. Ellison, M. K., and Scheidt, W. R. (1999) *J. Am. Chem. Soc. 121*, 5210−5219.
29. Slebodnick, C., and Ibers, J. A. (1997) *J. Biol. Inorg. Chem. 4*, 521−525.
30. Kachalova, G. S., Popov, A. N., and Bartunik, H. D. (1999) *Science 284*, 473−476.
31. Olson, J. S., and Phillips, G. N. (1997) *J. Biol. Inorg. Chem. 2*, 544−552.
32. Conti, E., Moser, C., Rizzi, M., Mattevi, A., Lionetti, C., Coda, A., Ascenzi, P., Brunori, M., and Bolognesi, M. (1993) *J. Mol. Biol. 233*, 498−508.
33. Bisig, D. A., Di Iorio, E. E., Diederichs, K., Winterhalter, K. H., and Piontek, K. (1995) *J. Biol. Chem. 270*, 20754−20762.
34. Springer, B. A., Sligar, S. G., Olson, J. S., and Phillips, G. N. (1994) *Chem. Rev. 94*, 699−714.
35. Tuckerman, J. R., Gonzalez, G., Dioum, E. M., and Gilles-Gonzalez, M.-A. (2002) *Biochemistry 41*, 6170−6177.

BI020144L